BIOCHEMISTRY
including biophysical chemistry & molecular biology

Article

pubs.acs.org/biochemistry

DXP Reductoisomerase: Reaction of the Substrate in Pieces Reveals a Catalytic Role for the Nonreacting Phosphodianion Group

Svetlana A. Kholodar and Andrew S. Murkin*

Department of Chemistry, University at Buffalo, The State University of New York, Buffalo, New York 14260, United States

Supporting Information

ABSTRACT: The role of the nonreacting phosphodianion group of 1-deoxy-D-xylulose-5-phosphate (DXP) in catalysis by DXP reductoisomerase (DXR) was investigated for the reaction of the "substrate in pieces". The truncated substrate 1-deoxy-L-erythrulose is converted by DXR to 2-*C*-methylglycerol with a k_{cat}/K_m that is 10^6-fold lower than that for DXP. Phosphite dianion was found to be a nonessential activator, providing 3.2 kcal/mol of transition state stabilization for the truncated substrate. These results implicate a phosphate-driven conformational change involving loop closure over the DXR active site to generate an environment poised for catalysis.

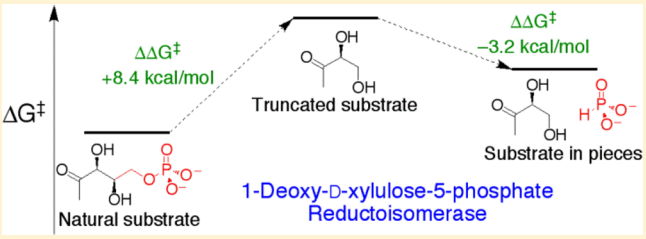

Survival of many bacteria, including major human pathogens such as *Mycobacterium tuberculosis*, largely depends on their ability to maintain biosynthesis of isoprenoids, essential metabolites derived from the five-carbon units isopentenyl pyrophosphate and dimethylallyl pyrophosphate. The pathway to isoprenoid biosynthesis in bacterial cells, known as the nonmevalonate or 2-*C*-methyl-D-erythritol 4-phosphate (MEP) pathway,[1] is independent of the mevalonate pathway present in animals;[2] thus, members of the MEP pathway present attractive targets for development of selective antibiotics with reduced toxicity to humans.

1-Deoxy-D-xylulose-5-phosphate (DXP) reductoisomerase (DXR) catalyzes the first committed step in the MEP pathway, involving a skeletal rearrangement of DXP via a retroaldol/aldol process,[3,4] followed by reduction by NADPH to yield MEP (Scheme 1).[5,6] Binding of DXP or the potent inhibitors

Scheme 1

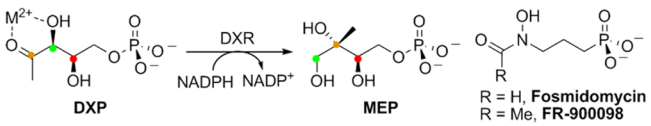

fosmidomycin and FR-900098 (Scheme 1) to DXR is achieved by two key interactions within the enzyme active site: (1) chelation by the oxygen atoms of the carbonyl and vicinal alcohol to the bound divalent metal cation (Mg^{2+}, Mn^{2+}, or Co^{2+}) and (2) electrostatic/H-bond interactions between the active site and the phosphate/phosphonate group. In addition to its role in ligand binding, the divalent metal, which is critical for steady-state turnover, is believed to stabilize the developing negative charge during the partially rate-limiting formation of the purported enediolate intermediate.[3] In contrast, the phosphoryl group, being remote from the reaction center, serves no obvious catalytic function. Studies have shown that removal of this group[7] or substitution with uncharged sulfone or sulfonamide groups[8] results in complete loss of substrate or inhibitor activity.[a] Substitution of a methylene group for the bridging oxygen (O-5) in DXP maintained activity but reduced its binding 4-fold.[9] Interestingly, Richard and co-workers have observed that whereas orotidine, the *dephosphorylated* version of the natural substrate, is a very poor substrate for orotidine-5′-monophosphate decarboxylase (OMPDC), removal of the *phosphorylmethyl* group stabilized the transition state by ∼3 kcal/mol.[10] This curious observation prompted us to adopt a "two-part" substrate strategy to investigate the role of the nonreacting phosphorylmethyl group in catalysis by DXR. By monitoring the reaction of the truncated substrate 1-deoxy-L-erythrulose (DE) in the presence and absence of phosphite dianion, we have quantified the contribution of the substrate's phosphorylmethyl group to catalytic efficiency and present a kinetic model featuring a critical dianion-driven protein conformational change.

EXPERIMENTAL PROCEDURES

Materials. All chemicals of analytical or reagent grade and were used without further purification unless otherwise stated. *E. coli* DXP synthase (DXS) was expressed and purified as reported[11] using its plasmid obtained as gifts from Prof. John S. Blanchard (Albert Einstein College of Medicine). *M. tuberculosis* DXR was cloned, expressed, purified, and quantified as reported previously.[12] *Thermoanaerobium brockii* alcohol dehydrogenase was purchased from Sigma-Aldrich. GC-MS analysis of 2-methylglycerol (2MG) and 1-methylglycerol

Received: January 24, 2013
Revised: March 5, 2013
Published: March 8, 2013

   dx.doi.org/10.1021/bi400092n | *Biochemistry* 2013, 52, 2302−2308

Table 1. Steady-State Kinetic Parameters for the DXP and DE Conversion by *Mt*DXR

kinetic parameter[a]	substrate		
	DXP[b]	DE	DE + HPO_3^{2-}
k_{cat} (s^{-1})	5.25 ± 0.19	0.00155 ± 0.00012	0.00086 ± 0.00006
K_m (mM)	0.115 ± 0.007	53 ± 5	53 ± 5
K_{HPi} (mM)	N/A	N/A	28 ± 4 (26 ± 4 of dianion[c])
k_{cat}/K_m (M^{-1} s^{-1})	(4.6 ± 0.3) × 10^4	0.0292 ± 0.018	0.163 ± 0.01

[a]Errors are standard errors from global fitting. [b]From Liu and Murkin.[12] [c]Calculated at pH 7.5, $pK_a(H_2PO_3^-)$ = 6.31 (determined from the pH of a 50 mM solution of sodium salt at 25 °C and I = 0.2 M (NaCl) at a 1:1 monoanion:dianion ratio).

(1MG) triacetates was performed using a Hewlett-Packard 5890 Series II gas chromatograph with 5972 mass selective detector and HP 7673 autosampler. ^{1}H NMR spectra were acquired on a Varian Mercury-300 spectrometer equipped with a broadband probe using default pulse sequences.

Synthesis of 1-Deoxy-L-erythrulose. DE was synthesized enzymatically by *Ec*DXS from pyruvate and glycolaldehyde.[13] The reaction mixture contained 50 mM glycolaldehyde, 50 mM sodium pyruvate, 1 mM thiamine pyrophosphate, 5 mM $MgCl_2$, 50 mM sodium phosphate buffer (pH 7.5), and 0.5 mg/mL *Ec*DXS. Reaction progress was monitored by ^{1}H NMR. Once the signals of starting material had depleted (ca. 24 h), the reaction was stopped by adding an equal volume of methanol and pelleting the enzyme. The supernatant was concentrated by rotary evaporation to produce a yellow oil, which was adsorbed onto silica gel and dry-loaded onto a silica gel column. Fractions were eluted with 5% methanol/CH_2Cl_2, identified by *p*-anisaldehyde staining, pooled, and concentrated by rotary evaporation. To remove UV contaminants, the residue was dissolved in water and passed through a 5 mL column of cellulose/activated charcoal (1:1), previously rinsed with 10% ethanol. The pooled DE fractions were concentrated to provide colorless oil that was dissolved in water and stored at 4 °C. ^{1}H NMR (300 MHz, 50% D_2O): δ 4.42 (t, J = 3.8 Hz, 1 H), 3.96 (dd, J = 12.3, 4.1 Hz, 1 H), 3.89 (dd, J = 12.3, 3.5 Hz, 1 H), 2.27 (s, 3 H). The concentration of the DE solution was determined through quantitative integration of its ^{1}H NMR signal using imidazole as an internal standard.[14] To ensure accurate integrals for the protons of interest, a relaxation delay between pulses of 120 s (>8T_1) was used.

***Mt*DXR-Catalyzed Synthesis of 2-*C*-Methylglycerol (2MG).** To demonstrate synthesis of 2-*C*-methylglycerol by *Mt*DXR in the presence of phosphite dianion, 100 μM *Mt*DXR was incubated in the presence of 40 mM DE, 10 mM NADPH, 10 mM $MgCl_2$, and 50 mM sodium phosphite buffer at pH 7.5 and 25 °C. Reaction progress was monitored by ^{1}H NMR. The ^{1}H NMR spectrum of the product of DE conversion was in agreement with that reported for 2-methyl-1,2,3-propanetriol prepared through chemical synthesis.[15] ^{1}H NMR (300 MHz, 20% D_2O): δ = 3.50 (s, 4H), 1.15 (s, 3H).

For the purpose of structure characterization by mass spectrometry, a second sample of 2MG was prepared enzymatically by *Mt*DXR from a reaction mixture containing 100 mM DE, 200 μM NADPH, 50 mM sodium phosphite buffer (pH 7.5), 10 mM $MgCl_2$, and 100 μM *Mt*DXR (dialyzed before use to remove glycerol). In order to recycle NADPH, 1 U/mL of $NADP^+$-dependent alcohol dehydrogenase from *T. brockii* and 2% (v/v) isopropyl alcohol were included (note: 1 U is the amount of enzyme required to reduce 1 μmol of $NADP^+$ per minute under these reaction conditions). The reaction mixture was incubated at 25 °C for 6 days, yielding 88% conversion of DE into 2-methylglycerol. Since *Mt*DXR was not stable during the reaction period, its addition (50 nmol) every 24 h was required to maintain conversion of DE to product. The reaction mixture was desalted by Amberlite IRA400 (OH^-) and Amberlite IR120 (H^+) ion exchange resins and passed through a 5 mL column of cellulose/activated charcoal (1:1), previously rinsed with 10% ethanol. The pooled 2MG fractions were concentrated to provide colorless oil that was dissolved in water and stored at 4 °C. Spectral data were in agreement with those previously reported.[15]

Chemical Synthesis of 2MG. The dimethyl acetal of 2MG was synthesized as reported previously.[16] 2MG was obtained by acid deprotection in the presence of Amberlite IR 120(H^+) in 95% ethanol upon refluxing at 80 °C for 2 h. The solution was passed through a 5 mL column of cellulose/activated charcoal (1:1), previously rinsed with 10% ethanol. The pooled 2MG fractions were concentrated to provide colorless oil that was dissolved in water and stored at 4 °C. The concentration of 2MG solution was determined by ^{1}H NMR with an imidazole internal standard as described above. Spectral data were in agreement with those previously reported.[15]

Acetylation of 2MG and 1MG Standards and Products of *Mt*DXR Turnover of DE. Acetylation of *Mt*DXR-generated products, chemically synthesized 2MG, and commercial 1MG was done according to published procedures[17,18] with modifications. Acetic anhydride (283 μL, 3 mmol) and $Er(OTf)_3$ (1 mg, 0.5 mol % vs 2MG) in acetonitrile (1 mL) were added to a neat 2MG, 1MG, or their mixture generated by *Mt*DXR (~0.3 mmol). Resulting mixture was stirred for 16 h at room temperature and then partitioned between CH_2Cl_2 (3 × 10 mL) and saturated $NaHCO_3$ (3 × 10 mL). The combined organic phase was washed with water, dried over Na_2SO_4, concentrated, and purified using flash silica gel chromatography (1:1 EtOAc/hexanes). Fractions containing triacetates (determined by ^{1}H NMR) were pooled and concentrated by rotary evaporation.

Steady-State Kinetics. Measurement of initial velocities was performed using an Applied Photophysics SX-20 stopped-flow spectrophotometer fit with a 20 μL flow cell (1 cm path length). The stopped-flow instrument was employed in preference to a conventional spectrophotometer primarily to reduce reactant quantities; unlike the reactions with the natural substrate DXP,[12] no additional kinetic events were observed within the initial second of detection. Final assay mixtures contained 0−50 mM sodium phosphite buffer (pH 7.5), 25 mM Tris-HCl buffer (pH 7.5), 10 mM $MgCl_2$, 10 mM DTT, 200 μM NADPH, 1.5−40 mM DE, and 2.5 μM *Mt*DXR at an ionic strength of 0.2 M adjusted with NaCl. Monitoring of the NADPH absorbance decay at 340 nm (ε_{340} = 6.22 mM^{-1} cm^{-1}) was performed at 25 °C for 200 s. The background velocity of the NADPH signal decay was determined at each phosphite concentration in the absence of DE (corresponding background velocities in the absence of enzyme were indistinguishable from

dx.doi.org/10.1021/bi400092n | *Biochemistry* 2013, 52, 2302−2308

those obtained in the absence of DE). The background velocities were in the range of 8−50% of the reaction rates in the presence of DE.

Data Analysis. Data were analyzed by analytical nonlinear regression using Pro-DataViewer (Applied Photophysics) and GraphPad Prism (GraphPad Software, La Jolla, CA), and standard errors associated with fitting are reported. Kinetic parameters presented in Table 1 were obtained by global fitting of eq 1 to the data.

$$\frac{v_0}{[E]} = \frac{(k_{cat}K_{HPi} + k'_{cat}[HPO_3^{2-}])[DE]}{[DE][HPO_3^{2-}] + K_m[HPO_3^{2-}] + K_{HPi}[DE] + K_mK_{HPi}} \quad (1)$$

RESULTS AND DISCUSSION

Analytical-scale formation of DE by condensation of pyruvate and glycolaldehyde catalyzed by DXP synthase (DXS; Scheme 2) was previously reported based on the analysis of reaction

Scheme 2

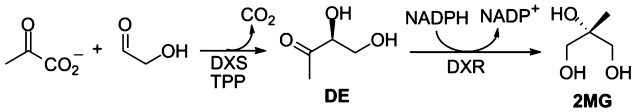

mixtures by HPLC with a refraction index detector.[13] We have confirmed the identity of the product by comparison of its ^{1}H NMR signals (Figure 1) to those reported for the chemically synthesized racemate.[19] Although the enantiomeric purity of enzymatically synthesized DE has not been directly established, it is assumed to have the same configuration as DXP and is therefore likely exclusively the L-isomer.

The predicted product of the *Mt*DXR-catalyzed reaction with DE is 2-*C*-methylglycerol (2MG), which differs from the natural product, MEP, by the absence of the phosphorylmethyl group (Scheme 2). To verify, *Mt*DXR (100 μM) was incubated with DE (40 mM), NADPH (10 mM), and Mg^{2+} (10 mM) in 50 mM sodium phosphite (pH 7.5, 47 mM dianion) at 25 °C for 24 h. The progress of the reaction was monitored by ^{1}H NMR (Figure 2) until NADPH had been depleted. The identity of the product was confirmed by preparation of a 2MG standard according to the published procedure.[16] The ^{1}H NMR spectrum of the *Mt*DXR-synthesized 2MG matched that of the standard, as did the GC-MS data of their acetylated derivatives (see Supporting Information). Interestingly, minor formation of 1-*C*-methylglycerol (1MG) was also observed during the course of *Mt*DXR turnover of DE. The ^{1}H NMR spectrum of this byproduct and GC-MS data of its acetylated derivative were in agreement with those of a commercially available sample of 1MG (see Supporting Information). Formation of 1MG indicates alteration of the specificity of the reduction step of the reaction upon dissection of the natural substrate into pieces. We speculate that the origin of the observed promiscuity is an altered conformation of the enzyme bound to the "two-part" substrate and/or an altered mode of substrate binding, but these possibilities will require further investigation.

The kinetics of *Mt*DXR-catalyzed reaction of DE was assayed by monitoring NADPH absorbance upon mixing a 1:1 volume ratio of solutions containing enzyme (2.5 μM final) and varying DE (0−40 mM final), respectively. Both solutions also contained saturating NADPH (200 μM) and varying phosphite dianion (0−50 mM), and a constant ionic strength of 0.2 M was maintained by addition of NaCl. The *Mt*DXR-catalyzed reaction with DXP follows a random ordered mechanism, though binding of NADPH first is preferential at 200 μM due to its low K_m (9.8 μM).[11,12] With DE as the substrate an even stronger preference for NADPH is expected due to the much higher K_m for the truncated ligand.

Initial rates were obtained by varying DE concentration (0−40 mM) at varying fixed concentrations of phosphite (0−50 mM; 0−47 mM dianion). The data revealed hyperbolic dependences on both ligands (Figure 3), consistent with a

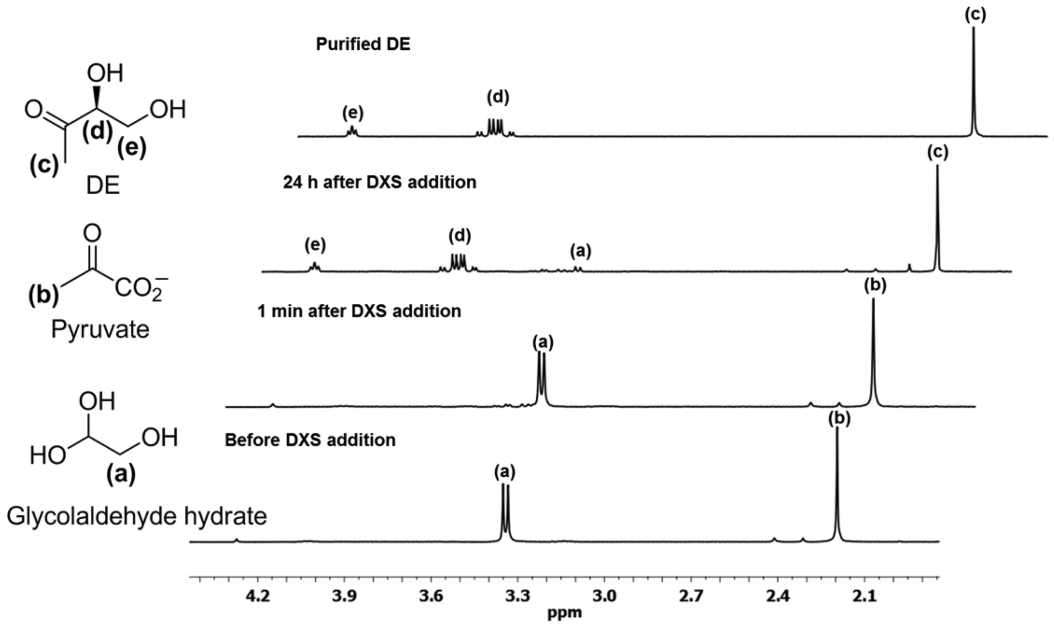

Figure 1. ^{1}H NMR monitoring of DXS-catalyzed condensation of glycolaldehyde and pyruvate to yield 1-deoxy-L-erythrulose (DE). Reaction conditions: 100 mM sodium pyruvate, 100 mM glycolaldehyde, 1 mM thiamine pyrophosphate, 5 mM $MgCl_2$, 50 mM sodium phosphate buffer (pH 7.5), 0.5 mg/mL DXS, 37 °C. Spectra were acquired in 50% D_2O at 300 MHz.

dx.doi.org/10.1021/bi400092n | *Biochemistry* 2013, 52, 2302−2308

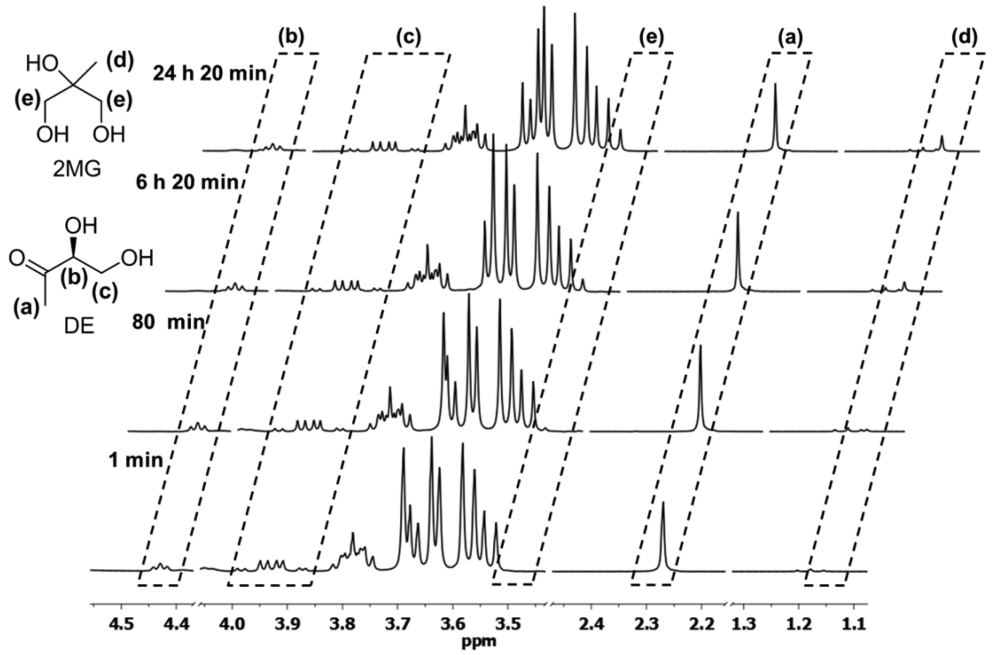

Figure 2. [1]H NMR monitoring of 2MG formation in the *Mt*DXR-catalyzed reaction with DE as a substrate in the presence of phosphite dianion. [1]H signals from DE include the methyl (H-1) at 2.27 ppm (a), methylene (H-4R and H-4S) at 3.89 and 3.96 ppm (b), and methine (H-3) at 4.42 ppm (c). Signals associated with ethanol (1.18 ppm), present in the commercial NADPH, and with glycerol (3.50−3.83 ppm) and Tris (3.69 ppm), present in the *Mt*DXR storage buffer, are also detectable at the initiation of the reaction. Turnover of DE results in the appearance of a singlet at 1.15 ppm due to the methyl group of 2MG (d) and a singlet at 3.50 ppm due to the methylene groups (e). Reaction conditions: 100 μM *Mt*DXR, 40 mM DE, 10 mM NADPH, 10 mM $MgCl_2$, 50 mM sodium phosphite buffer, pH 7.5, 25 °C. Spectra were acquired in 50% D_2O at 300 MHz, with suppression of the HDO peak by presaturation.

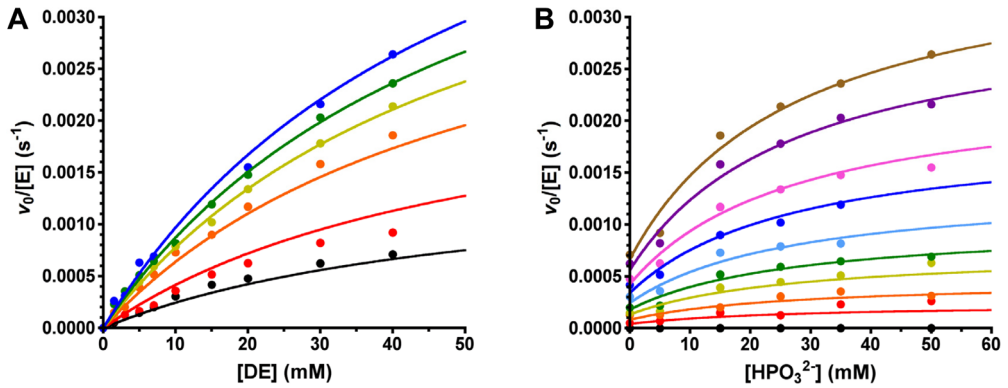

Figure 3. Dependence of the rate of *Mt*DXR-catalyzed DE turnover on the (A) concentrations of DE ([HPO_3^{2-}] from bottom to top: 0, 1.5, 3.0, 5.0, 7.0, 10, 15, 20, 30, and 40 mM) and (B) phosphite dianion ([DE] from bottom to top: 0, 4.7, 14.1, 23.5, 32.9, and 47.0 mM) at pH 7.5, 25 °C (I = 0.2 M, NaCl).

nonessential activation model (Scheme 3)[20] for the observed activation of *Mt*DXR by phosphite dianion. In this scheme, k_{cat} and k_{cat}' are the first-order rate constants in the absence and presence of phosphite, respectively, and the K_m of DE and the dissociation constant of phosphite (K_{HPi}) are independent of the presence of the other ligand. The first- and second-order rate constants as well as K_m and K_{HPi} (Table 1) were obtained by global fitting of the rate equation (eq 1)[20] to the data.

Scheme 3

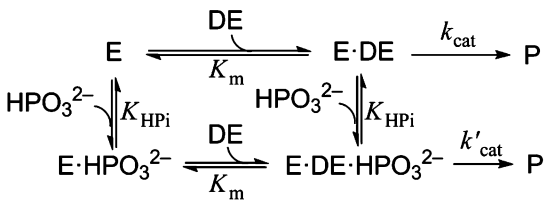

Truncation of DXP led to a drastic drop in the first- and second-order rate constants. While k_{cat} was reduced over 3000-fold from 5.25 s^{-1}, k_{cat}/K_m was lowered by 6 orders of magnitude from 4.6×10^4 M^{-1} s^{-1}, reflecting a large increase in K_m (over 400-fold).[12] The reduction in both k_{cat} and k_{cat}/K_m upon truncation emphasizes the importance of the phosphate group as not only an anchoring determinant but also a group promoting the chemical steps through ground-state destabilization and/or transition-state stabilization. Assuming that the reactions involving DXP and DE share the same rate-limiting step, the decrease in the second-order rate constant upon removal of the phosphorylmethyl group indicates that the

dx.doi.org/10.1021/bi400092n | *Biochemistry* 2013, 52, 2302−2308

transition state for reaction of DXP is stabilized by 8.4 kcal/mol (using eq 2) by interactions between *Mt*DXR and the nonreacting phosphate (Table 2). This intrinsic phosphate

Table 2. Comparison of Intrinsic Phosphate (ΔG_{Pi}) and Phosphite (ΔG_{HPi}) Binding Energies and Conformational Free Energy for the Reaction of Truncated Substrates Catalyzed by DXR, TIM, OMPDC, and GPDH

	intrinsic binding energy, kcal/mol			conformational energy, kcal/mol
enzyme (source)	ΔG_{Pi}[a]	ΔG_{HPi}[b]	$\Delta G_{HPi} - \Delta G_{Pi}$	$E_o \rightleftharpoons E_c$ (ΔG_C)
DXR (*M. tuberculosis*)	−8.4	−3.2	5.4	1.0
TIM (rabbit muscle)[c]	−12.2	−5.8	6.4	3.9
OMPDC (yeast)[d]	−11.8	−7.8	4.0	6.6
GPDH (rabbit muscle)[c]	≤−11.0	−7.7	≥3.3	6.3−7.7

[a]Calculated at 298 K using eq 2. [b]Calculated at 298 K using eq 3. [c]From Tsang et al.[24] [d]From Amyes et al.[23]

binding energy is 3−4 kcal/mol lower in magnitude than those determined for the unrelated reactions catalyzed by triosephosphate isomerase (TIM),[14,21,22] OMPDC,[23] and glycerol-3-phosphate dehydrogenase (GPDH)[24] (Table 2). Unlike these other enzymes, however, DXR additionally utilizes a metal cofactor to orient the substrate and stabilize the transition state. Consequently, whereas the phosphodianion presumably contributes a substantial portion of the total binding energy of the transition states for TIM, OMPDC, and GPDH, the total binding energy associated with the transition state for DXR is balanced between the interactions at both ends of the molecule.

The presence of saturating concentrations of phosphite increased the first- and second-order rate constants for the *Mt*DXR-catalyzed reaction with DE by a factor of 5.5 (Table 1). Using eq 3 with K_{HPi} = 26 mM, this yields an intrinsic *phosphite* binding energy of −3.2 kcal/mol. Although this is 3−4 kcal/mol lower in magnitude than the corresponding values measured for TIM, OMPDC, and GPDH, the *difference* in phosphate and phosphite intrinsic binding energies of 5.4 kcal/mol falls within the range observed for these enzymes (Table 2). This energy difference largely reflects the entropic penalty paid for binding the substrate as two pieces instead of one.[25]

$$\Delta G_{Pi} = -RT \ln\left[\frac{(k_{cat}/K_m)_{DXP}}{(k_{cat}/K_m)_{DE}}\right] \quad (2)$$

$$\Delta G_{HPi} = -RT \ln\left[\frac{k'_{cat}/K_m}{(k_{cat}/K_m)K_{HPi}}\right] \quad (3)$$

To appreciate the significance of DXR activation by phosphite dianion, it is useful to consider the model previously invoked for TIM, OMPDC, and GPDH.[26] Supported by crystallographic evidence,[27−29] a conformational equilibrium exists between open and closed forms of the enzyme, the latter of which is catalytically active. In the closed conformation a flexible so-called "phosphate gripper loop" interacts with the phosphate group of the ligand and serves to order and sequester the active site from bulk solvent. Similar interactions of this loop with phosphite dianion have been proposed to stabilize the closed conformation, thus leading to the observed activation of the reaction with the "substrate in pieces". Parallels can be drawn with DXR by inspection of crystal structures of its complexes with fosmidomycin, FR-900098, and their analogues,[30−33] which suggest crucial roles for the phosphonate group in binding, orientation, and induction of conformational changes. Most significantly, upon inhibitor binding a flexible loop consisting of residues 198−206 of *Mt*DXR,[33] 291−299 of *Plasmodium falciparum* DXR (*Pf*DXR),[34] and 207−215 of *Escherichia coli* DXR (*Ec*DXR, not shown)[35] undergoes a ∼16 Å movement to close over the active site (Figure 4). A histidine

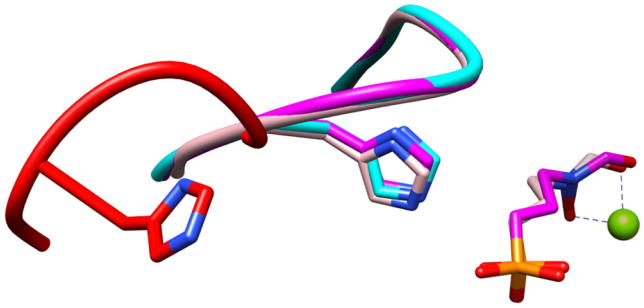

Figure 4. The flexible loop of DXR complexes, featuring the histidine residue that interacts with bound dianion. The loop has been colored red for *Pf*DXR·Mn^{2+}·NADPH (PDB 3AU8),[34] pink for *Pf*DXR·Mg^{2+}·NADPH·FOM (PDB 3AU9),[34] magenta for *Mt*DXR·Mn^{2+}·NADPH·FOM (PDB 4AIC),[31] and cyan for *Mt*DXR·Mn^{2+}·NADPH·SO_4^{2-} (PDB 2JD1).[31] The metal ion is green.

residue (*Mt*DXR, His200; *Pf*DXR, His293; *Ec*DXR, His209) within this loop forms a key interaction with one of the phosphonate/phosphate oxygens. Interestingly, the presence of sulfate dianion alone in the phosphate-binding pocket of *Mt*DXR resulted in adoption of the loop-closed conformation (Figure 4, cyan),[30] suggesting that interactions involving the phosphoryl group or its analogue are solely responsible for the observed protein rearrangement.

The observed phosphite activation of the *Mt*DXR-catalyzed reaction of the substrate in pieces can be rationalized by Scheme 4. Consistent with models described for the other three

Scheme 4

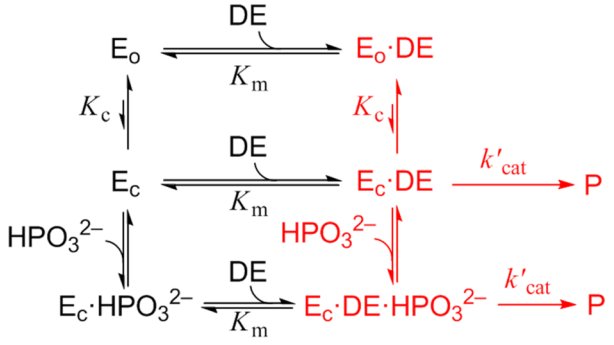

phosphite-activated enzymes,[26] this scheme features a conformational equilibrium between a predominant, inactive open form (E_o) and a minor, active closed form (E_c) of the unliganded enzyme. The proposed role of the phosphite dianion is to shift the equilibrium toward the active form upon binding. Accordingly, it is assumed that E_c and E_c·HPO_3^{2-} exhibit the same reactivity toward the truncated substrate such that $k_{cat} = K_c k'_{cat}$ and $k_{cat}/K_m = K_c k'_{cat}/K_m$. Interestingly, unlike with TIM and OMPDC, saturation of *Mt*DXR could be

dx.doi.org/10.1021/bi400092n | *Biochemistry* 2013, 52, 2302−2308

demonstrated with the truncated substrate. The fact that the DE-saturated enzyme remains activated by phosphite dianion (Figure 3) indicates that the Michaelis complex must include the open enzyme form (red pathway in Scheme 4) and that binding of DE does not alter the conformational equilibrium. With an observed phosphite activation factor of 5.5, K_c = 0.18, which corresponds to a free energy barrier of only 1.0 kcal/mol (Table 2 and Figure 5). In contrast, TIM, OMPDC, and GPDH exhibit much larger conformational energy barriers, up to ∼7 kcal/mol. Thus, whereas the majority of the intrinsic phosphite binding energy for these enzymes is expended in mobilizing the "phosphate gripper loop", only about 1/3 of this energy is used to drive the flexible loop in *Mt*DXR.

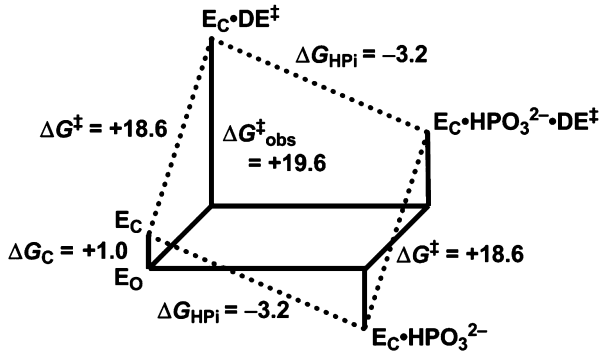

Figure 5. Free energy profile (not to scale) for phosphite-activated turnover of DE catalyzed by the loop-closed form of *Mt*DXR. The unbound ligand(s) at each vertex has been omitted for clarity. The labeled values are free energy changes in kcal/mol, calculated from the kinetic parameters in Tables 1 and 2 using a 1 M substrate standard state. Under saturating DE conditions, only the magnitudes of $\Delta G^{\ddagger}$ and $\Delta G^{\ddagger}_{obs}$ are changed.

Consistent with the hypothesis that a phosphoryl group or a close analogue are required for inducing the loop conformational change that strengthens interactions between the enzyme and ligand, studies involving fosmidomycin analogues with its phosphonate group replaced by isosteric functionalities such as sulfonate, carboxylate, and tetrazole reported significantly diminished inhibition.[36,37] These findings indicate substantial specificity of the phosphate/phosphonate-binding pocket for the geometric and hydrogen-bonding/electrostatic properties of its ligand. Interestingly, Deng and co-workers[38] exploited this requirement by preserving the phosphonate group while introducing α lipophilic groups that participate in interactions with the conserved histidine residue of the flexible loop. Of particular note in their study, lipophilic phosphonates lacking the hydroxamate group present in fosmidomycin were found to be moderately effective inhibitors of *Ec*DXR (IC_{50} as low as 840 nM), suggesting that the phosphonate dianion is a more significant determinant for binding than the metal-chelating hydroxamate. Taken together with the phosphite activation in the current study, these observations underscore the importance of interactions between the functional groups of the ligand and residues of the flexible loop, which may be critical for the design of potent inhibitors.

The low rates of both the reaction of the truncated substrate and "substrate in pieces" may be due to nonoptimal positioning of the substrate in the active site or an inability of the enzyme to attain exactly the same closed conformation that is generated in the presence of the natural substrate; the observation of the minor alternative product supports these possibilities. Both of these outcomes could significantly influence transition-state stabilization, leading to a large increase of at least one of the chemical barriers: isomerization and/or reduction. Structural and kinetic isotope effect studies are underway to probe these factors.

■ ASSOCIATED CONTENT

Ⓢ Supporting Information

^{1}H NMR and GC-MS data. This material is available free of charge via the Internet at http://pubs.acs.org.

■ AUTHOR INFORMATION

Corresponding Author

*E-mail amurkin@buffalo.edu, Ph (716) 645-4249.

Funding

This work was supported by funds from the University at Buffalo.

Notes

The authors declare no competing financial interest.

■ ACKNOWLEDGMENTS

We thank Drs. Tina Amyes and John Richard (University at Buffalo) for helpful discussions.

■ ABBREVIATIONS

1MG, 1-*C*-methylglycerol (1,2,3-butanetriol); 2MG, 2-*C*-methylglycerol (2-methylpropane-1,2,3-triol); DE, 1-deoxy-L-erythrulose; DXP, 1-deoxy-D-xylulose 5-phosphate; DXR, 1-deoxy-D-xylulose-5-phosphate reductoisomerase; DXS, 1-deoxy-D-xylulose-5-phosphate synthase; GPDH, glycerol-3-phosphate dehydrogenase; MEP, 2-C-methyl-D-erythritol 4-phosphate; $NADP^+$, oxidized form of nicotinamide adenine dinucleotide phosphate; NADPH, reduced form of nicotinamide adenine dinucleotide phosphate; OMPDC, orotidine-5′-monophosphate decarboxylase; TIM, triosephosphate isomerase.

■ ADDITIONAL NOTE

[a]In light of the high K_m determined for DE in the present study, it is possible that the absence of observable activity with 2 mM 1-deoxy-D-xylulose is attributable to a high K_m.

■ REFERENCES

(1) Grawert, T., Groll, M., Rohdich, F., Bacher, A., and Eisenreich, W. (2011) Biochemistry of the non-mevalonate isoprenoid pathway. *Cell. Mol. Life Sci. 68*, 3797−3814.

(2) Miziorko, H. M. (2011) Enzymes of the mevalonate pathway of isoprenoid biosynthesis. *Arch. Biochem. Biophys. 505*, 131−143.

(3) Manning, K. A., Sathyamoorthy, B., Eletsky, A., Szyperski, T., and Murkin, A. S. (2012) Highly precise measurement of kinetic isotope effects using 1H-detected 2D [13C,1H]-HSQC NMR spectroscopy. *J. Am. Chem. Soc. 134*, 20589−20592.

(4) Munos, J. W., Pu, X., Mansoorabadi, S. O., Kim, H. J., and Liu, H. W. (2009) A secondary kinetic isotope effect study of the 1-deoxy-D-xylulose-5-phosphate reductoisomerase-catalyzed reaction: evidence for a retroaldol-aldol rearrangement. *J. Am. Chem. Soc. 131*, 2048−2049.

(5) Proteau, P. J. (2004) 1-Deoxy-D-xylulose 5-phosphate reductoisomerase: an overview. *Bioorg. Chem. 32*, 483−493.

(6) Kuzuyama, T., Takahashi, S., Takagi, M., and Seto, H. (2000) Characterization of 1-deoxy-D-xylulose 5-phosphate reductoisomerase, an enzyme involved in isopentenyl diphosphate biosynthesis, and identification of its catalytic amino acid residues. *J. Biol. Chem. 275*, 19928−19932.

(7) Takahashi, S., Kuzuyama, T., Watanabe, H., and Seto, H. (1998) A 1-deoxy-D-xylulose 5-phosphate reductoisomerase catalyzing the formation of 2-C-methyl-D-erythritol 4-phosphate in an alternative nonmevalonate pathway for terpenoid biosynthesis. *Proc. Natl. Acad. Sci. U. S. A. 95*, 9879−9884.
(8) Perruchon, J., Ortmann, R., Altenkamper, M., Silber, K., Wiesner, J., Jomaa, H., Klebe, G., and Schlitzer, M. (2008) Studies addressing the importance of charge in the binding of fosmidomycin-like molecules to deoxyxylulosephosphate reductoisomerase. *ChemMedChem 3*, 1232−1241.
(9) Phaosiri, C., and Proteau, P. J. (2004) Substrate analogs for the investigation of deoxyxylulose 5-phosphate reductoisomerase inhibition: synthesis and evaluation. *Bioorg. Med. Chem. Lett. 14*, 5309−5312.
(10) Goryanova, B., Spong, K., Amyes, T. L., and Richard, J. P. (2013) Catalysis by orotidine 5′-monophosphate decarboxylase: Effect of 5-fluoro and 4′-substituents on the decarboxylation of two-part substrates. *Biochemistry 52*, 537−546.
(11) Argyrou, A., and Blanchard, J. S. (2004) Kinetic and chemical mechanism of Mycobacterium tuberculosis 1-deoxy-D-xylulose-5-phosphate isomeroreductase. *Biochemistry 43*, 4375−4384.
(12) Liu, J., and Murkin, A. S. (2012) Pre-steady-state kinetic analysis of 1-deoxy-D-xylulose-5-phosphate reductoisomerase from *Mycobacterium tuberculosis* reveals partially rate-limiting product release by parallel pathways. *Biochemistry 51*, 5307−5319.
(13) Schurmann, M., Schurmann, M., and Sprenger, G. A. (2002) Fructose 6-phosphate aldolase and 1-deoxy-D-xylulose 5-phosphate synthase from *Escherichia coli* as tools in enzymatic synthesis of 1-deoxysugars. *J. Mol. Catal. B: Enzym. 19*, 247−252.
(14) Amyes, T. L., and Richard, J. P. (2007) Enzymatic catalysis of proton transfer at carbon: activation of triosephosphate isomerase by phosphite dianion. *Biochemistry 46*, 5841−5854.
(15) Bongini, A., Cardillo, G., Orena, M., Porzi, G., and Sandri, S. (1982) Regiocontrolled and stereocontrolled synthesis of epoxy alcohols and triols from allylic and homoallylic alcohols via iodo carbonates. *J. Org. Chem. 47*, 4626−4633.
(16) Forbes, D. C., Ene, D. G., and Doyle, M. P. (1998) Stereoselective synthesis of substituted 5-hydroxy-1,3-dioxanes. *Synthesis*, 879−882.
(17) Smith, M. E. B., Hibbert, E. G., Jones, A. B., Dalby, P. A., and Hailes, H. C. (2008) Enhancing and reversing the stereoselectivity of *Escherichia coli* transketolase via single-point mutations. *Adv. Synth. Catal. 350*, 2631−2638.
(18) Procopio, A., Dalpozzo, R., De Nino, A., Maiuolo, L., Russo, B., and Sindona, G. (2004) Erbium(III) triflate as an extremely active acylation catalyst. *Adv. Synth. Catal. 346*, 1465−1470.
(19) Kis, K., Volk, R., and Bacher, A. (1995) Biosynthesis of riboflavin. Studies on the reaction mechanism of 6,7-dimethyl-8-ribityllumazine synthase. *Biochemistry 34*, 2883−2892.
(20) Segel, I. H. (1975) *Enzyme Kinetics: Behavior and Analysis of Rapid Equilibrium and Steady State Enzyme Systems*, Wiley, New York.
(21) Richard, J. P. (2012) A paradigm for enzyme-catalyzed proton transfer at carbon: triosephosphate isomerase. *Biochemistry 51*, 2652−2661.
(22) Amyes, T. L., O'Donoghue, A. C., and Richard, J. P. (2001) Contribution of phosphate intrinsic binding energy to the enzymatic rate acceleration for triosephosphate isomerase. *J. Am. Chem. Soc. 123*, 11325−11326.
(23) Amyes, T. L., Richard, J. P., and Tait, J. J. (2005) Activation of orotidine 5′-monophosphate decarboxylase by phosphite dianion: the whole substrate is the sum of two parts. *J. Am. Chem. Soc. 127*, 15708−15709.
(24) Tsang, W. Y., Amyes, T. L., and Richard, J. P. (2008) A substrate in pieces: allosteric activation of glycerol 3-phosphate dehydrogenase (NAD+) by phosphite dianion. *Biochemistry 47*, 4575−4582.
(25) Jencks, W. P. (1981) On the attribution and additivity of binding energies. *Proc. Natl. Acad. Sci. U. S. A. 78*, 4046−4050.
(26) Amyes, T. L., and Richard, J. P. (2013) Specificity in transition state binding: The Pauling model revisited. *Biochemistry*, DOI: 10.1021/bi301491r.
(27) Noble, M. E., Zeelen, J. P., and Wierenga, R. K. (1993) Structures of the "open" and "closed" state of trypanosomal triosephosphate isomerase, as observed in a new crystal form: implications for the reaction mechanism. *Proteins 16*, 311−326.
(28) Callahan, B. P., and Miller, B. G. (2007) OMP decarboxylase−An enigma persists. *Bioorg. Chem. 35*, 465−469.
(29) Ou, X., Ji, C., Han, X., Zhao, X., Li, X., Mao, Y., Wong, L. L., Bartlam, M., and Rao, Z. (2006) Crystal structures of human glycerol 3-phosphate dehydrogenase 1 (GPD1). *J. Mol. Biol. 357*, 858−869.
(30) Henriksson, L. M., Bjorkelid, C., Mowbray, S. L., and Unge, T. (2006) The 1.9 A resolution structure of *Mycobacterium tuberculosis* 1-deoxy-D-xylulose 5-phosphate reductoisomerase, a potential drug target. *Acta Crystallogr., Sect. D: Biol. Crystallogr. 62*, 807−813.
(31) Henriksson, L. M., Unge, T., Carlsson, J., Aqvist, J., Mowbray, S. L., and Jones, T. A. (2007) Structures of *Mycobacterium tuberculosis* 1-deoxy-D-xylulose-5-phosphate reductoisomerase provide new insights into catalysis. *J. Biol. Chem. 282*, 19905−19916.
(32) Andaloussi, M., Henriksson, L. M., Wieckowska, A., Lindh, M., Bjorkelid, C., Larsson, A. M., Suresh, S., Iyer, H., Srinivasa, B. R., Bergfors, T., et al. (2011) Design, synthesis, and X-ray crystallographic studies of alpha-aryl substituted fosmidomycin analogues as inhibitors of *Mycobacterium tuberculosis* 1-deoxy-D-xylulose 5-phosphate reductoisomerase. *J. Med. Chem. 54*, 4964−4976.
(33) Bjorkelid, C., Bergfors, T., Unge, T., Mowbray, S. L., and Jones, T. A. (2012) Structural studies on Mycobacterium tuberculosis DXR in complex with the antibiotic FR-900098. *Acta Crystallogr., Sect. D: Biol. Crystallogr. 68*, 134−143.
(34) Umeda, T., Tanaka, N., Kusakabe, Y., Nakanishi, M., Kitade, Y., and Nakamura, K. T. (2011) Molecular basis of fosmidomycin's action on the human malaria parasite Plasmodium falciparum. *Sci. Rep. 1*, 9.
(35) Mac Sweeney, A., Lange, R., Fernandes, R. P., Schulz, H., Dale, G. E., Douangamath, A., Proteau, P. J., and Oefner, C. (2005) The crystal structure of *E. coli* 1-deoxy-D-xylulose-5-phosphate reductoisomerase in a ternary complex with the antimalarial compound fosmidomycin and NADPH reveals a tight-binding closed enzyme conformation. *J. Mol. Biol. 345*, 115−127.
(36) Zingle, C., Kuntz, L., Tritsch, D., Grosdemange-Billiard, C., and Rohmer, M. (2010) Isoprenoid biosynthesis via the methylerythritol phosphate pathway: structural variations around phosphonate anchor and spacer of fosmidomycin, a potent inhibitor of deoxyxylulose phosphate reductoisomerase. *J. Org. Chem. 75*, 3203−3207.
(37) Nguyen-Trung, A. T., Tritsch, D., Grosdemange-Billiard, C., and Rohmer, M. (2013) Synthesis of tetrazole analogues of phosphonohydroxamic acids: An attempt to improve the inhibitory activity against the DXR. *Bioorg. Med. Chem. Lett. 23*, 1643−1647.
(38) Deng, L., Endo, K., Kato, M., Cheng, G., Yajima, S., and Song, Y. (2011) Structures of 1-deoxy-D-xylulose-5-phosphate reductoisomerase/lipophilic phosphonate complexes. *ACS Med. Chem. Lett. 2*, 165−170.